

# Analysis of Mechanical Stress Associated with Trench Isolation using a Two-Dimensional Simulation

S. Matsuda, N. Itoh, C. Yoshino, Y. Tsuboi, Y. Katsumata, and H. Iwai

ULSI Laboratories, Research and Development Center, Toshiba Corporation  
1, Komukai-Toshiba-cho, Saiwai-ku, Kawasaki, Japan  
Phone: +81-44-549-2183 Fax: +81-44-549-2290

## Introduction

Oxide-filled trench structures have been introduced both into high-speed bipolar LSIs and also into high-density CMOS devices. In these applications, shallow or deep trenches are used, and sometimes a combination of both types. Such trenches not only reduce the isolation area but also effectively reduce parasitic capacitances as a result of the thick oxide layer they contain. Thus, the trench structure is essential not only from the point of view of higher density, but also for reasons of speed. While trench isolation has great merits, it sometimes leads to problems caused by mechanical stress; the trenches are filled with oxide using a high-temperature deposition process, so great mechanical stress is generated by thermal coefficient differentials during the subsequent substrate cooling process. This stress distorts the silicon area, as shown in Fig.1, and sometimes leads to defects in the silicon itself; the result may be significant leakage current at the junctions, such as between the base and collector or drain and substrate. The degree of mechanical stress depends on the trench configuration. For example, the distance between the edges of shallow and deep trenches, indicated in Fig.2, significantly affects the junction leakage current as shown in Fig.3. In this paper, we report on a technique of stress analysis around trenches based on a two-dimensional finite element simulation.

## Mechanical Stress Simulation

Assuming that the deformation is elastic, the strain,  $\epsilon$ , and stress,  $\sigma$ , are given by the following equations:

$$\epsilon = \alpha(T) (T - T^i), \quad \epsilon_{yy}/\epsilon_{xx} = -\nu, \quad \sigma = E \epsilon$$

where  $\alpha$  is the coefficient of thermal expansion,  $T$  is the final temperature,  $T^i$  is the initial temperature,  $E$  is Young's modulus, and  $\nu$  is Poisson's ratio. The material constants for components used in the simulation are listed in Table 1. The boundary conditions and initial conditions are given in Fig. 4.

Figure 5 shows the simulated displacements around the trench in magnified form. The stress distribution calculated from these displacement is shown in Fig.6(a). These are Tresca's equivalent stress which is defined as the difference between maximum and minimum principal stress. The actual stress distribution in a sample can be measured by micro-Raman spectroscopy, and the simulated distribution and magnitude was verified to agree with the measurements over all [1]. In general, junctions are located in relatively shallow regions, so the stress distribution in the shallow region was thought to have most influence on the electrical characteristics of a device. Within this smaller region of the surface, there still seems to be good agreement between the simulation, shown in Fig.6(a) and the measurements, shown in Fig.6(b). The measurements, however, have poor resolution in this area, because the diameter of the laser beam used in Raman spectroscopy is  $0.7 \mu\text{m}$  the same order as the junction depth. On the other hand, the simulated results give good enough resolution for a detailed analysis of the stress distribution in this area, so this method of simulation is a very useful way to analyze the effect of stress on electrical characteristics.

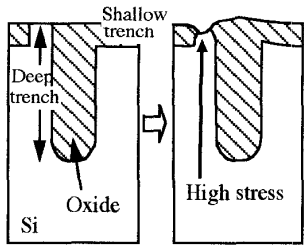
Figure 7 shows simulated stress distributions for various trench configurations. Contrary to the anticipation from the leakage current data shown in Fig.3, there was not so much difference, due to the configuration, in the stress distributions near the surface region where the junction lies. The stress distributions along the junction shown in Fig.8 indicate even slightly larger maximum stress values in a case where there is a certain distance between the shallow and deep trench edges (case(a)). It should be noted, however, that the stress distribution in the deeper region is very much different among the samples as shown in Fig. 9. In case (c), where the shallow and deep trench edges abut each other, the stress is great in a large area in the deeper region. This is the great contrast to the other cases also as shown in Fig. 10. From Figs. 7-10, it is obvious that the stress in the deeper region is governed by the distance between the deep trenches. This is supported by the result that the stress is reduced significantly even in case (e) for  $L = 0 \mu\text{m}$  if the distance between the deep trenches is large ( $6.6 \mu\text{m}$ ). Thus, it is estimated that the stress in the deeper region induces defects near the junction or depletion region, and distances between the deep trench is an important factor for the junction leakage current.

These simulations assume an oxide deposition temperature of  $650^\circ\text{C}$ . The stress can be reduced significantly by using a lower deposition temperature, as shown in Fig 11. The dependence of stress on the deep trench spacing is shown in the figure. Stress increases significantly as the spacing is reduced, but it can be relieved by reducing the deposition temperature. Thus it is very important to reduce the process temperature as much as possible in future ULSI generations, not only because this suppresses impurity diffusion but also because it reduces the leakage current resulting from mechanical stress.

## Conclusion

Two-dimensional mechanical stress simulation was applied to the junction leakage current analysis of the trench isolated devices. It was shown that the simulation is a very useful tool not only for analysis but also investigation of possible problems associated with new structures and prevent them.

[1] Y. Katsumata, et al., IEEE BCTM, p271, 1991



High temperature Low temperature  
 Fig. 1 Schematic of stress inducement in LSI process

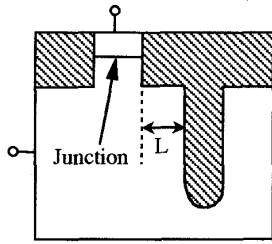


Fig. 2 Schematic cross section of trench isolation

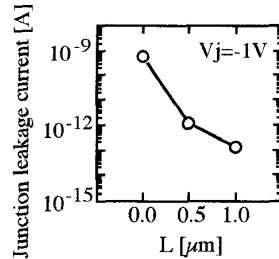


Fig. 3 Junction leakage current as a function of L.

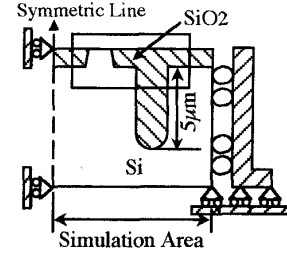


Fig. 4 Simulation structure model

Table 1. Material constants for various films

	Young's modulus [N/m <sup>2</sup> ]	Poisson's ratio	Thermal expansion coefficient [1/°C]
Si	1.59x10 <sup>-1</sup>	0.36	2.3x10 <sup>-6</sup>
SiO <sub>2</sub>	7.24x10 <sup>-2</sup>	0.45	5.5x10 <sup>-7</sup>

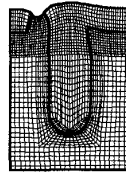


Fig. 5 Displace of stress simulated mesh magnified 300 times

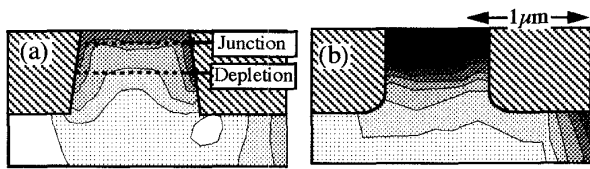
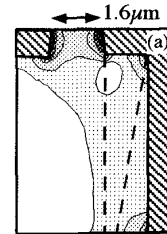
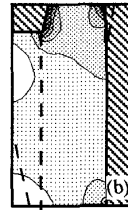


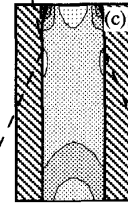
Fig. 6 Simulated and measured stress distribution around trench isolation.  
 (a) Simulated  
 (b) Measured by Raman microprobe technique



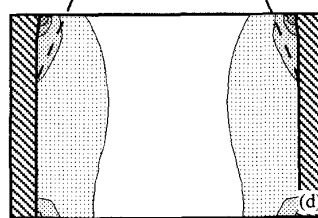
Lactive=1.6 μm  
 LTR=6.6 μm



Lactive=1.6 μm  
 LTR=4.6 μm



Lactive=LTR=1.6 μm



Lactive=LTR=6.6 μm

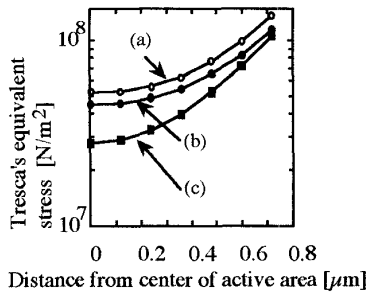


Fig. 8 Simulated lateral stress distribution of active region (0.2 μm depth)

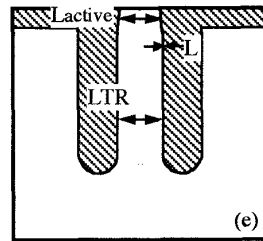


Fig. 7 Simulated stress distribution at 650°C. (a) L=1 μm, (b) L(one side)=0 μm, (c) L(both sides)=0 μm, and (d) large dimension isolation

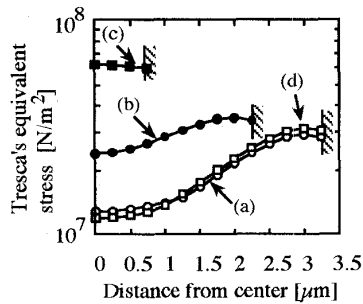


Fig. 9 Simulated lateral stress distribution of deeper region (4 μm depth)

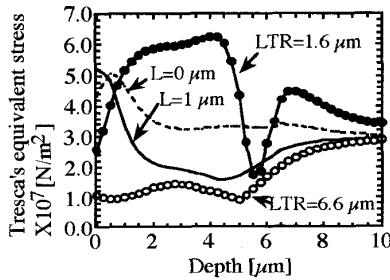


Fig. 10 Depth profile of stress at center of active region for various structures

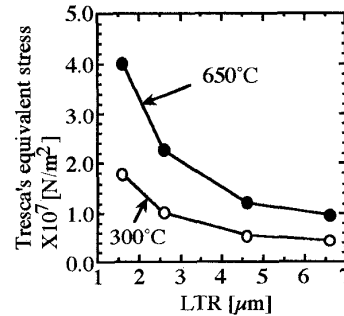


Fig. 11 Stress at center of active region as functions of LTR